Remote Sensing of Environment 196 (2017) 265–278

Contents lists available at ScienceDirect

Remote Sensing of Environment

journal homepage: www.elsevier.com/locate/rse

Biomass estimation in a boreal forest from TanDEM-X data, lidar DTM, and the interferometric water cloud model

Jan I.H. Askne *, Maciej J. Soja, Lars M.H. Ulander

Department of Earth and Space Sciences, Chalmers University of Technology, SE-412 96 Gothenburg, Sweden

ARTICLE INFO

Article history:
Received 31 October 2016
Received in revised form 22 April 2017
Accepted 8 May 2017
Available online 20 May 2017

Keywords:
Boreal forest
Biomass
Forest height
TanDEM-X
InSAR
ALS

ABSTRACT

The semi-empirical Interferometric Water Cloud Model, IWCM, is used to estimate above ground forest biomass, AGB, in northern Sweden, Krycklan (64°N 20°E). The results are based on separate analysis of 14 TanDEM-X acquisitions from 2011 to 2014 and a Lidar digital terrain model (DTM). 29 stands covering 272 ha and with AGB < 183 Mg/ha, and 619 stands with area > 1 ha covering 3166 ha and with AGB < 291 Mg/ha have been analyzed. In situ and airborne lidar scanning, ALS, data from the BioSAR 2008 experiment are used as reference. AGB and forest height are estimated using a new optimization method for determining IWCM parameters. Allometric equations are used to describe the inter-dependency between forest height, biomass, area-fill factor, and stem volume. No local training data from the investigated area are used to determine model parameters. For the 29 stands, the relative RMSE for biomass estimated using the proposed method varied between 15.8% and 21.2% (r^2 between 0.82 and 0.88) and between 9.9% and 16.0% for height (r^2 between 0.84 and 0.89). Dependence of model parameters on temperature and precipitation as well as height of ambiguity are investigated. A method based on look-up table for biomass estimation from phase height is proposed. The method is used over an area of 68 km^2 for one TanDEM-X acquisition from 2011-06-04 and the results are compared with an ALS biomass map from August 2008. Good agreement is observed, as well as high potential for clear-cut detection.

1. Introduction

A third of the Earth's land is covered by forests and around 30% of the forested area consists of boreal forests. In Sweden 51% is covered by productive forest of mainly boreal or hemi-boreal type. Forests are one of the major sinks in the global carbon cycle (Houghton et al., 2009), and play an important role in Swedish economy. An important variable in carbon cycle models is above-ground biomass, AGB, and different remote sensing methods have been developed to estimate AGB and AGB change. However, forest properties are complex, especially in tropical areas, and there is no satellite technique able to measure forest AGB globally. Radars operating in the low VHF and UHF bands are useful due to their improved penetration capabilities and sensitivity to larger branches and stem properties, and a P-band (432–428 MHz) synthetic aperture radar (SAR) satellite mission, BIOMASS, is under development by ESA (ESA, 2012; Le Toan et al., 2011).

No remote sensing technique can measure AGB directly. Sensitivity to the canopy with leaves, needles, and branches, and to tree stems, including moisture content, and sensitivity to the ground, soil type, moisture and topography vary with frequency. The backscattering at low radar frequencies (typically, VHF-band and P-band) is sensitive to major AGB components, i.e. stems and large branches, which is not the case for high radar frequencies (typically, C- and X-band). However, the latter can serve as a complement, in particular for less dense forests, since the backscattering relationship to AGB at low frequencies is complex and is also affected by ground and soil properties. High radar frequencies are mainly sensitive to the upper parts of the canopy and then to the height of the forest, which is closely related to biomass, although the vegetation density is also of major importance for AGB estimation. The relationship between the interferometric phase height and forest height based on 3-day repeat-pass C-band data was studied in Askne et al. (1997) and Ulander et al. (1994). It was found that the phase height depends not only on forest height but also on the vegetation density or the gaps in the vegetation. For the analysis, the Interferometric Water Cloud Model, IWCM, was introduced (Askne et al., 1997). The temporal decorrelation and atmospheric artifacts associated with ERS repeat pass data made height measurements unreliable (Santoro et al., 2005). The bistatic configuration of TanDEM-X effectively eliminates the temporal decorrelation and atmospheric artifacts and makes possible accurate height and AGB estimates, see e.g. Askne et al. (2013), Askne and Santoro (2015), Kaasalainen et al. (2015), Karila et al. (2015), Kugler et al. (2014), Persson and Fransson (2016), Soja et al. (2015a), Soja et al. (2015b), Solberg et al. (2013), Toraño Caicoya et al. (2016), Toraño Caicoya et al. (2015), and Treuhaft et al. (2015), as

* Corresponding author at: Chalmers University of Technology, Department of Earth and Space Sciences, SE-412 96 Gothenburg, Sweden.
E-mail address: jan.askne@chalmers.se (J.I.H. Askne).

http://dx.doi.org/10.1016/j.rse.2017.05.010

long as a Digital Terrain Model, DTM, is available, which is becoming more and more common.

C-band and X-band are usually considered less useful for AGB estimation based on backscatter. This is due to saturation at relatively low biomass, and due to sensitivity to soil and vegetation moisture. However, it has been shown that with the hyper-temporal BIOMASAR method (Santoro et al., 2015; Santoro et al., 2011) good results can be obtained even with C-band backscatter data, but at a coarse resolution. Moreover, with ERS-1/2 C-band repeat pass information it was shown that coherence can give high accuracy estimates for certain weather conditions (Askne and Santoro, 2012; Santoro et al., 2002).

TanDEM-X, launched in June 2010, is a twin satellite to TerraSAR-X for single pass interferometry based on a phase synchronization link and tightly controlled formation flying. It is the first bistatic SAR satellite mission, operating at X-band, with a center frequency of 9.65 GHz and a wavelength of 3.1 cm (Krieger et al., 2007). The primary objective is to acquire the first, fully global digital elevation model, DEM. In forested areas, the phase center is shifted to a height related to the forest height and density (Askne et al., 1997). With a DTM available from e.g. airborne lidar scanning, ALS, it becomes possible to determine the phase height relative to the ground level, and the phase height can be related to the forest height and indirectly also to AGB.

This article will deal with the application of TanDEM-X observations to boreal forests, focusing on a boreal test area, the Krycklan river catchment (Lat 64°16′N Long. 19°46′E) in northern Sweden, Fig. 1, and applying the Interferometric Water Cloud Model, IWCM (Askne et al., 1997; Askne and Santoro, 2012; Askne et al., 2013; Askne and Santoro, 2015; Santoro et al., 2002), for analysis of the interferometric SAR observations. The phase height and the coherence of the signal are observed together with the backscatter. Since the phase height is determined by tree heights as well as the vegetation density and the biomass is closely related to these two properties, the interferometric height is also closely related to biomass (Askne et al., 1997; Hagberg et al., 1995; Soja et al., 2015a; Solberg et al., 2010b). Before TanDEM-X, important X-band InSAR results regarding forest height and biomass were also demonstrated using data from the SRTM mission e.g. Solberg et al. (2010a), Sun and Ranson (2009).

Solberg et al. (2013) studied two TanDEM-X acquisitions from a spruce dominated site in southeast Norway and found an almost linear relation between AGB and phase height with a slope of 14 tons/ha/m. Askne et al. (2013) studied 18 acquisitions from the hemi-boreal site Remningstorp in Sweden using the Interferometric Water Cloud Model, IWCM, and also found an almost linear relation between phase height and biomass, but with a varying slope. Treuhaft et al. (2015) studied a tropical site based on one TanDEM-X acquisition and related biomass to phase height and coherence by multiple regression, a technique also used by Persson and Fransson (2016) for studies of one TanDEM-X scene from each of Krycklan and Remningstorp. Karila et al. (2015) studied five TanDEM-X pairs from an area in southern Finland using the Random-Forest approach. Soja et al. (2015a) used a two level method (TLM) to determine biomass from Krycklan with ten pairs and from Remningstorp with eight pairs. All presented results using TanDEM-X single polarization and different analysis methods have shown high accuracy for biomass estimation with Root Mean Square Errors (RMSE) of the order of 15–25% at stand level. Krycklan or areas close by have also been observed in many other remote sensing experiments using P-, L-, C- and X-band with forest biomass or height as a goal, and the TanDEM-X results are among the best in comparison (Askne and Santoro, 2012; Kugler et al., 2014; Neumann et al., 2012; Persson and Fransson, 2014; Persson et al., 2013; Soja et al., 2015a; Soja et al., 2013; Tebaldini and Rocca, 2012).

The above mentioned papers as well as an earlier analysis of TanDEM-X acquisitions from Remningstorp (Askne et al., 2013) used local training data to determine the model parameters. Remote sensing, in the meaning of the words, means that we want to avoid a demand of a large set of stands with known forest properties in order to calibrate/train the inversion model, although reference stands should be used to validate the results of the investigation. Recently a method was presented on how to avoid local training data (Askne and Santoro, 2015) and the analysis will now be extended to a dataset from Krycklan by means of a new optimization method.

The paper is organized as follows. The test site is first introduced followed by a presentation of the TanDEM-X data and the associated meteorological data. The Interferometric Water Cloud Model is presented followed by methods for solution, results for AGB and forest height estimation and validation for forest stands with in situ data. Finally the results are extended to a large area for which ALS data are available and the results are discussed and conclusions made.

2. Site properties

The test site is located in the Krycklan river catchment (Lat 64°16′N Long. 19°46′E) in northern Sweden and covers approximately 68 km^2. It is a topographic area with ground elevation varying between 145 m and

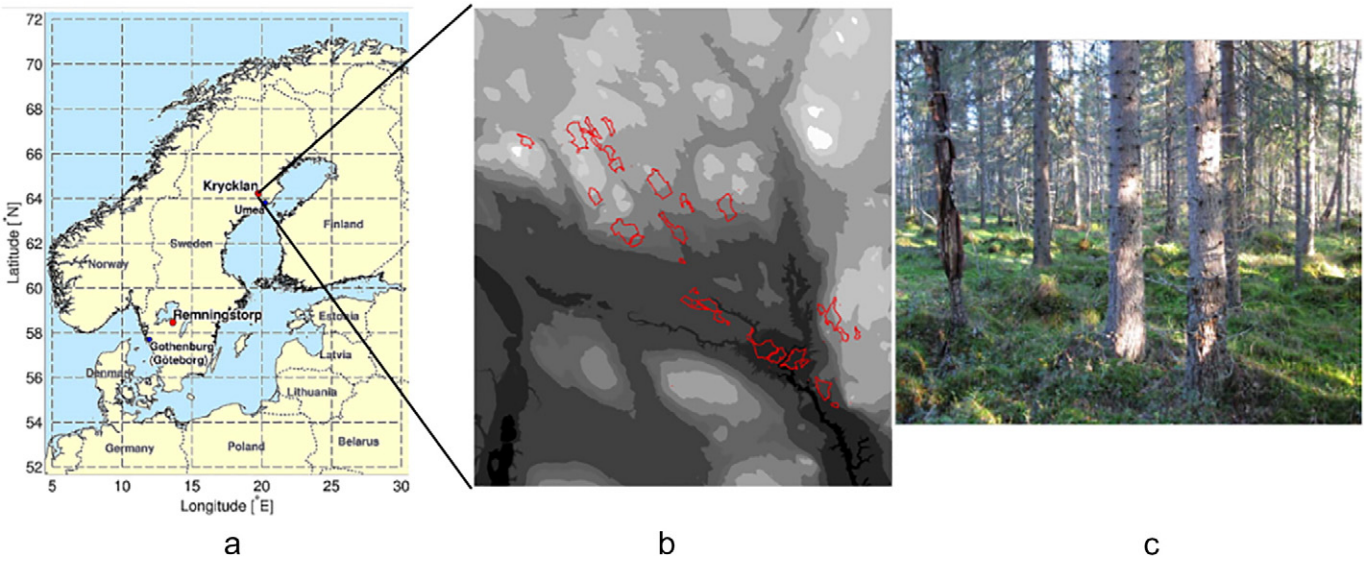

Fig. 1. a) The test site Krycklan. (Remningstorp 720 km away also illustrated) b) DTM illustrating altitudes 145–400 m in steps of 36 m together with contours of the stands used in this paper with in situ information. c) Stand 2269, biomass 183 Mg/ha, average ground slope 5°. The sun on the ground illustrates the gap in the vegetation, from Hajnsek et al. (2009).

400 m above sea level. Slopes measured on a 50 m × 50 m grid varies up to 19° but are locally much steeper, e.g. along the river gorges. The forest consists mainly of Norway spruce (*Picea abies* (L.) Karst.), Scots pine (*Pinus sylvestris* L.), and birch (*Betula* spp.).

Ground data were collected and processed as part of the BioSAR campaign in 2008 (Hajnsek et al., 2009). A set of 31 forest stands (see Fig. 1), covering low to high biomass values as well as a few ground slope classes, were selected for in situ measurements. The stands were established to ensure a uniform stratification with respect to slope, and biomass based on an ALS (airborne laser scanning) survey conducted in 2006 with ground slopes computed over 80 m × 80 m units and estimates of stem volume. These 31 forest stands varied in size between 1.2 and 23.8 ha (after removal of a 5-m buffer zone). Within each stand, 8–13 circular field plots (10 m radius) were laid out with a systematic spacing of 50 to 160 m, depending on the size of the area. The spacing in each stand was determined with the aim of obtaining ca 10 plots. For each field plot, all trees with a diameter at breast height (dbh at 1.3 m above ground) larger than 4 cm were calipered and tree species were identified. Tree height and age were measured on sample trees, randomly selected within each field plot with a probability proportional to basal area, resulting in an average of 1.5 sample trees per field plot. Additional field plot variables were also collected, e.g. site index. AGB (including stem, bark, branches and leaves/needles, but excluding stump and roots; mass per unit area in Mg/ha) for each stand was calculated based on Petersson's biomass functions (Petersson, 1999). Fig. 1 illustrates one of the stands with an area of 16.1 ha and average values: dbh 28 cm, age 122 years, 869 stems/ha, basal area 38.5 m^2/ha, stem volume 380 m^3/ha and biomass 182 Mg/ha. The photo in Fig. 1 also illustrates the gaps in the vegetation with the sun illuminating the ground. The standard error for the estimated biomass varied between 4 and 21% which was computed based on the number of field plots within each stand and the variation between plots within each stand.

In addition to the 31 stands with in situ data, a new stand delineation map of Krycklan was produced based on aerial photography and new ALS data collected in 2008. The size of the stands varied between 0.04 and 57.3 ha. The laser returns were classified as ground or vegetation returns, and a DTM was derived using the laser returns classified as ground returns. The laser (vegetation) height was determined as the difference to the DTM below. A height threshold of 10% of the maximum laser height and laser height ≥ 1.0 m was applied in order to separate canopy returns from returns of e.g. stones and low vegetation. Laser height percentiles, 10, 20, …, 90, 95 and 100%, were determined on a 10 m × 10 m grid as the height at a given percentage of laser returns from the canopy. AGB was estimated using regression modeling: $\ln(AGB) = a + b \cdot P + c \cdot Veg + \varepsilon$, where P is the best performing height percentile of the ALS data and *Veg* is the vegetation ratio, i.e. the proportion of ALS measurements exceeding 1 m above ground or 10% of the maximum height. The three coefficients were determined using the field plots within the 31 stands, together with additional 110 circular field plots positioned in the central part of the Krycklan area. For more details about the field data and analysis, see Hajnsek et al. (2009), and Holmgren (2004).

Of the original 31 stands two were clear cut in the meantime between 2008 and 2011. In the following only the remaining 29 stands are used for comparison between TanDEM-X results and field and ALS inventory, while all 31 stands are illustrated in order to illustrate the effect of clear cuts in TanDEM-X images. Fig. 2 illustrates measured values over the 31 stands.

3. TanDEM-X data and meteorological data

A very large number of TanDEM-X acquisitions are available for Krycklan, due to it being a boreal forest reference site. The fourteen acquisitions analyzed in this paper are all from orbit 9 with an incidence angle of 41°, passing over Krycklan at 16:12 UTC. The first acquisition is from 2011-06-17 and features dual-pol, VV and VH polarizations, but the remaining acquisitions are single-pol, featuring only VV polarization. Only VV polarization is investigated in this paper. All acquisitions available for this orbit are included, which means a large span of meteorological conditions while at the same time the angle of incidence is constant. The height of ambiguity (the height interval for which the interferometric phase increases from 0 to 2π), HoA, varied between 36 and 136 m. Ten of the acquisitions have been analyzed in Soja et al. (2015a) using the Two Level Model, TLM, one has been analyzed in Persson and Fransson (2016), and two have been analyzed in Toraño Caicoya et al. (2016). For a description of processing of the TanDEM-X data used in this paper, see Soja et al. (2015a).

Studying the TanDEM-X data for stands we find that the phase height varies from 0 to 17.2 m and most of the phase height observations show very stable properties with typically $r^2 = 0.99$ between different acquisitions but for the two winter observations, 2012-02-25 with 1 m snow layer and −9 °C, for which r^2 versus the other observations are in the range 0.85 to 0.94 (highest value for r^2 is obtained between the two winter acquisitions). For the backscatter values we find r^2 of the order 0.97 but with low values, 0.44–0.8 when 2011-08-22 and 2012-02-25 are involved. The coherence varied between 0.25 and 0.94 and r^2 between 0.49 and 0.94 with the lowest r^2 for 2012-02-25 and 2013-12-27 relative the rest. This means that the phase height showed the best temporal stability in comparison with coherence and backscatter between acquisitions except between summer and winter cases. The difference between winter and summer cases may be related to temperature and moisture affecting vegetation dielectric constant, the effect of leaf loss, and differences caused by snow.

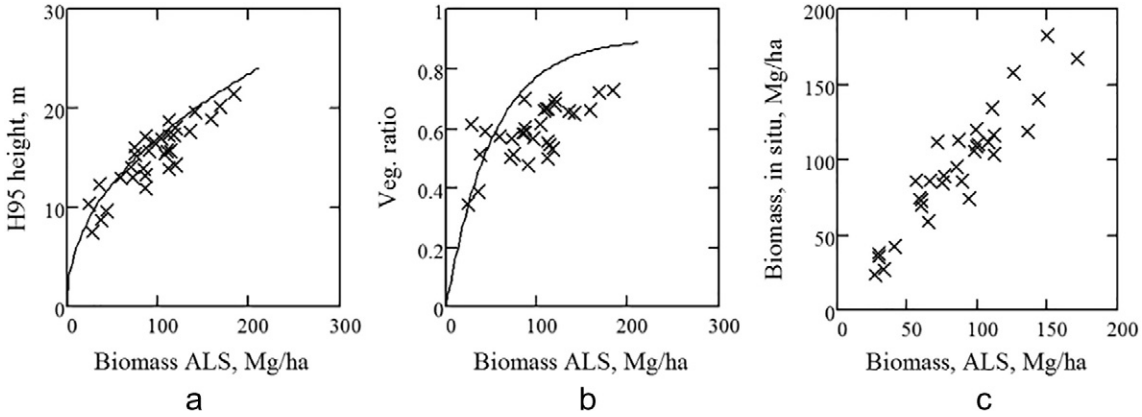

Fig. 2. Examples of ground data from the 31 stands. The two allometric equations used in this paper, Eqs. (6) and (7), are shown as solid lines in a) together with the ALS H95 vs. ALS biomass and b) ALS vegetation ratio (area-fill, η) vs. ALS biomass, and in c) In situ biomass vs. ALS biomass.

The high correlation of the measurements over time with the exceptions of 2012-02-25 and 2013-12-27 (having a snow layer, see Table 1) is illustrated in Fig. 3, where the first and last summer acquisitions (2011-06-17 and 2014-08-26) are plotted against each other.

TanDEM-X data were acquired on the dates listed in Table 1 together with the meteorological information from the site available from the Swedish Meteorological and Hydrological Institute, temperature, snow layer, and precipitation. Precipitation is also given for a three-day period.

4. Interferometric water cloud model

The semi-empirical Interferometric Water Cloud Model, IWCM, is based on models for backscattering coefficient, coherence and phase height (Askne et al., 1997; Askne and Santoro, 2012; Askne and Santoro, 2015; Santoro et al., 2002). Backscatter is determined as in the water cloud model (Attema and Ulaby, 1978), but generalized to include gaps in the vegetation cover by the introduction of the area-fill η, the area fraction covered by vegetation

$$\sigma^0_{for} = \eta\left[\sigma^0_{gr}e^{-\alpha h} + \sigma^0_{veg}\left(1-e^{-\alpha h}\right)\right] + (1-\eta)\sigma^0_{gr} \tag{1}$$

where σ^0_{gr} is ground backscattering coefficient (−), σ^0_{veg} is vegetation layer backscattering coefficient (−), h is the height of the layer of random scatterers (m), and α is the attenuation coefficient (m^{-1}).

The complex coherence of the random volume with gaps is then modeled by IWCM, which includes terms for volume decorrelation and for temporal and system decorrelation (Askne et al., 2003; Santoro et al., 2002). For bistatic observations, with zero along track baseline, the temporal decorrelation can be neglected, resulting in:

$$\bar{\gamma} = \gamma_{\mathrm{sys}}\frac{\bar{\gamma}_{vol} + m}{1+m} \tag{2}$$

where γ_{sys} is the zero height coherence, γ_{vol} is the volume decorrelation (Askne et al., 1997; Rodriguez and Martin, 1992), determined by α and h, and m is the ground-to-volume scattering ratio:

$$\bar{\gamma}_{vol} = \frac{\int_0^h e^{-\alpha(h-z')}\cdot e^{-j\mathrm{k}_z z'}\,\mathrm{d}z'}{\int_0^h e^{-\alpha(h-z')}\,\mathrm{d}z'} = \frac{\alpha}{\alpha - j\mathrm{k}_z}\frac{e^{-j\mathrm{k}_z h} - e^{-\alpha h}}{1-e^{-\alpha h}} \tag{3}$$

$$m = \frac{\sigma^0_{gr}}{\sigma^0_{veg}}\frac{1-\eta\left(1-e^{-\alpha h}\right)}{\eta\left(1-e^{-\alpha h}\right)} \tag{4}$$

where $k_z = 2\pi/\mathrm{HoA}$ and HoA is the height of ambiguity. From Eq. (2) the phase height, i.e. the height of the phase center, z_{est}, and coherence, γ, are determined by

$$\gamma = |\bar{\gamma}| \tag{5a}$$

$$z_{est} = -\frac{HoA}{2\pi}\arg(\bar{\gamma}) \tag{5b}$$

The IWCM is a semi-empirical model using radiative transfer theory to model penetration through the partially transparent canopy and geometrical optics to model penetration through canopy gaps. The unknown model parameters $\alpha, \sigma^0_{gr}, \sigma^0_{veg,}$ and γ_{sys} are assumed to be spatially invariant constants with the first three describing the properties of a certain forest type over a large area. Of the three modeled quantities (γ, z_{est}, and σ^0_{for}), z_{est} is a function of α and $\sigma^0_{gr}/\sigma^0_{veg}$. γ is also dependent on γ_{sys}, whereas σ^0_{for} is dependent on α, σ^0_{gr}, and σ^0_{veg}. The vertical and horizontal structures of the forest are in the model described by h and η.

4.1. Forest properties used as constraints

The area-fill is closely coupled to canopy closure, which is a common concept in optical remote sensing and can be measured by hemispherical photos (Santoro et al., 2002), ALS observations of the vegetation fraction (Holmgren et al., 2003; Korhonen et al., 2011; Lefsky et al., 2002; Næsset, 2002), or by satellite data (Cartus and Santoro, 2016; Cartus et al., 2012; Cartus et al., 2011). Also, it has been shown that the two-level model (TLM) can be used together with TanDEM-X data and a lidar digital terrain model (DTM) to measure a metric closely related to canopy closure without the need for reference data (Soja et al., 2015b).

The area-fill can be modeled in a similar way as it is done for canopy cover (Li and Strahler, 1985; Liu et al., 2008), i.e., as one minus an exponential function of both stand density and crown area. In the present paper, we will assume a relation for $\eta(V)$ expressed as:

$$\eta(V) = \eta_\infty\left(1-e^{-\lambda_0 V}\right) \tag{6}$$

where V is the stem volume and η_∞, and λ_0 are factors representing the maximum value of the area-fill and the increase with V. We will here use $\eta_\infty = 0.9$, and $\lambda_0 = 0.01$ ha/m^3, factors representative for the hemi-boreal test site Remningstorp (Askne and Santoro, 2015). For very large V, one might expect $\eta = 1$, but in practice the expression saturates at lower levels for high stem volumes, which is supported by

Table 1
Meteorological data from Vindeln-Sunnansjönäs (Lat 64°8′N Long. 19°46′E) at 237 m above sea level for the dates of TanDEM-X acquisitions with height of ambiguity, HoA (courtesy SMHI, http://opendata-download-metobs.smhi.se/explore/).

Date	HoA m	Temp 06/18 UTC, °C	min/max temp 18 – 18 UTC °C	Snow layer 06 UTC, cm	Prec./24 h 06 UTC, mm	Prec./72 h 6 UTC, mm
2011-06-17	52.05	14.5/12.7	8.9/19.8	0	0	0
2011-07-20	54.11	14.7/17.2	12.8/23.2	0	0	3.4
2011-08-11	55.50	8.6/11.2	6.7/13.2	0	0.9	1.1
2011-08-22	56.35	14.3/13.3	11.5/15.5	0	27.5	27.5
2012-02-25	79.41	−4.5/−8.9	−9.2/−3.3	102	8.3	5.5
2012-07-17	36.13	12.4/16.4	6.8/18.8	0	0	9.9
2012-08-08	37.49	11.1/12.1	6.1/17.8	0	0	1.8
2012-08-19	38.52	12.7/10.1	10.1/17.8	0	0	0.7
2013-06-01	49.97	17.7/14.9	12.4/23.1	0	1.8	1.8
2013-06-23	51.67	14.1/16.6	12.6/20.9	0	0	7.2
2013-07-26	62.25	19.1/20.8	12.0/27.0	0	0	0
2013-12-27	135.94	−1.3/−0.1	−1.8/0.3	6	3.8	7.4
2014-07-13	37.57	17.7/21.0	10.3/25.3	0	0	0
2014-08-26	69.12	9.9/12.4	8.2/16.3	0	0	27.5

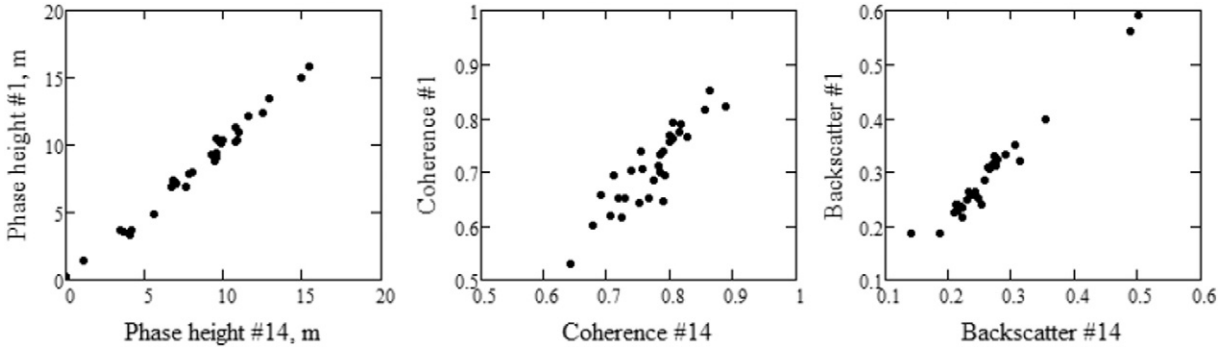

Fig. 3. Comparison of the first and last acquisitions, i.e. 2011-06-17 (#1) and 2014-08-26 (#14), for the 31 stands.

observations in Askne et al. (2013), Cartus and Santoro (2016), Cartus et al. (2012), and Cartus et al. (2011). Note that $\eta(V)$ is the area-fill at X-band, and averaged over the stand. $\eta(V)$ is expected to be higher than the canopy cover observed at optical frequencies and ALS since the gaps have to be larger at X-band than optical frequencies for the waves to pass through and also due to the angle of incidence.

Forest height is used with different meanings. The basal area weighted forest mean height is often used by foresters to describe the dominant height. (It should be noted that the basal area weighted mean height is a property dependent on tree heights and basal areas but not on density.) In ALS applications, forest height is often quantified using different height percentiles (commonly 95th and 99th percentiles). In studies related to height estimation from PolInSAR data, e.g. Mette et al. (2004), the H100 metric is used, defined as the mean height of the 100 tallest trees per hectare. The height used in the IWCM model is defined as the height of the random volume, and in this article, it will be assumed to be equal to the in situ-measured basal area weighted mean forest height and also compared with ALS-based height metric H95 (the 95th percentile of lidar returns classified as vegetation returns, i.e. height exceeding 1 m above ground or 10% of the maximum height in a 10 m × 10 m grid cell).

Expression (6) introduced stem volume as the forest variable, but the primary quantity in Eqs. (1) to (5b) is the observation of forest height. However, an allometric relation is useful between basal area weighed mean forest height and stem volume

$$h(V) = (\mathrm{a} \cdot V)^{\mathrm{b}} \tag{7}$$

For Swedish forests (Askne et al., 1997; Askne and Santoro, 2012) we have a = 2.44, and b = 0.46, where h is the basal area weighted mean forest height (m) and V the stem volume (m^3/ha). Allometric relations between height and stem volume (or biomass) are quite common for different forest types, e.g. Siberian forests (Santoro et al., 2007), temperate forests (Mette et al., 2004), and forests in north-eastern USA (Cartus et al., 2012). (It should be noted that allometric relations, $h(V)$ and $\eta(V)$, are statistical in nature and do not specifically take effects related to e.g. a thinning or a clear cut with seed trees into account.)

Using Eqs. (6) and (7), IWCM can be re-formulated as a function of stem volume. However, there is a high correlation between stem volume and biomass for different tree species, e.g. Thurner et al. (2013), and with a certain mixture between tree species the following model for biomass estimation from stem volume will be used:

$$B = BF\,V \tag{8}$$

where BF is a Biomass Factor, relating stem volume to AGB (excluding stumps). For Remningstorp, $BF = 0.512$ Mg/m^3 was used in (Askne et al., 2013). In this paper, the same values for η_∞, β_0, and BF are chosen for Krycklan as for Remningstorp, situated 720 km south-southwest of Krycklan, in order to avoid site-specific factors. The allometric models are illustrated in Fig. 2.

The aforementioned allometric functions relate forest variables h, η, V, and B to each other and reduce the number of unknown forest parameters to one. With three observables (σ^0_{for}, γ, and z_{est}) for each forest stand, the forest variable associated with each stand as well as the four spatially invariant IWCM parameters are estimated from the data. Methods to solve IWCM without local training data have been demonstrated in Askne and Santoro (2015), and a new method will also be demonstrated in the next section.

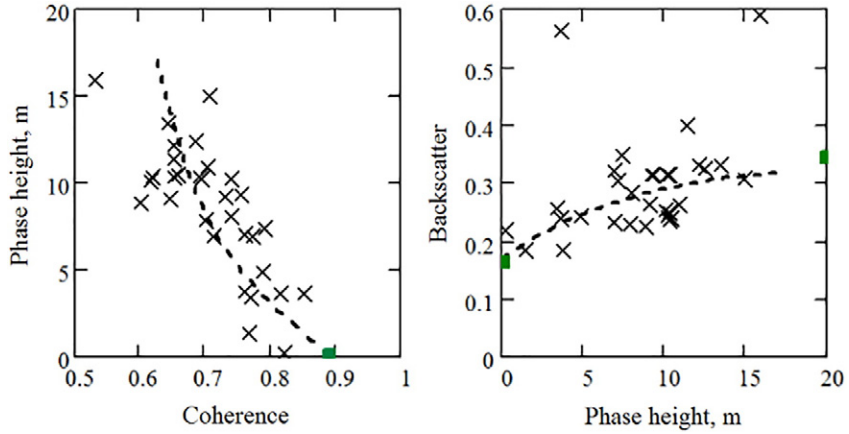

Fig. 4. Illustrating 31 observations from 2011-06-17, and derived model, plotted versus each other. γ_{sys}, σ^0_{gr}, and σ^0_{veg} are marked by filled green squares.

4.2. Estimation of IWCM parameters

We will here present a new method for IWCM fitting to experimental data, related to the solution presented in Askne and Santoro (2015), but now fully automatic.

The observations of phase height, H_i, coherence, C_i, and backscatter, $S_i = \sqrt{S_{1,i}S_{2,i}}$, where $S_{1,i}$ and $S_{2,i}$ are backscatter coefficient observations from each of the two satellites and the index i refers to each of the stands, are illustrated in Fig. 4 for one TanDEM-X acquisition from 2011. The backscattering coefficients have been computed by normalizing with the ground resolution cell (Ulander, 1996). Using the allometric relation (7), the height variable in IWCM is expressed as a function of stem volume. Parameters σ^0_{gr} and γ_{sys} correspond to backscatter and coherence for stem volume equal to zero, whereas parameter σ^0_{veg} corresponds to backscatter intensity for complete canopy cover, $\eta = 1$, and $\alpha h \gg 1$. The phase height typically increases with stem volume V, so first estimates of $\sigma^0_{gr}, \sigma^0_{veg}$, and γ_{sys} can be obtained by analyzing backscatter and coherence for low and high phase height values, see Fig. 4. Besides the IWCM parameters, $\alpha, \sigma^0_{gr}, \sigma^0_{veg}$, and γ_{sys}, assumed spatially invariant, the stem volumes, V_i, for all stands are also unknown.

Since the phase height varies over a large range in relation to the spread of the observations and a large number of looks is used during phase height estimation, we will neglect the uncertainty in phase height estimation and equate the IWCM phase height model z_{est} to the observed phase height, H_i. The coherence and backscatter models are used to obtain estimates of model parameters α, γ_{sys}, σ^0_{gr}, and σ^0_{veg}, which thereafter will be used to obtain the stem volume, biomass, and height estimates for each stand.

We first solve for the stem volumes V_i [or height expressed by Eq. (7)] as a function of the observed phase height and (so far unknown) values for $\alpha, \sigma^0_{gr}, \sigma^0_{veg}$, and γ_{sys}. (Note that the phase height is only dependent on $\alpha, \sigma^0_{gr}/\sigma^0_{veg}$, and V_i - the dependence on HoA is, for simplicity, suppressed in the following equation, but should nevertheless be noted.)

$$z_{est}\left(\alpha, \sigma^0_{gr}/\sigma^0_{veg} V_i\right) - H_i = 0 \tag{9}$$

Following the discussion from the previous paragraph, it is here assumed that all variations in H_i can be modeled with $z_{est}(\alpha, \sigma^0_{gr}/\sigma^0_{veg}, V_i)$. From Eq. (9) we obtain a function for stem volume estimation such that $V_i = V(\alpha, \sigma^0_{gr}/\sigma^0_{veg}, H_i)$. With this expression for V_i we use coherence and backscatter to estimate the model parameters $\alpha, \sigma^0_{gr}, \sigma^0_{veg}$, and γ_{sys} by minimizing the summed squares of the differences between the modeled and measured values of coherence and backscatter for all N stands:

$$\Delta\gamma\left(\alpha, \sigma^0_{gr}, \sigma^0_{veg}, \gamma_{sys}\right) = \sqrt{\frac{1}{N}\sum_{i=1}^{N}\left[\gamma\left(\alpha, \frac{\sigma^0_{gr}}{\sigma^0_{veg}}, \gamma_{sys}, V\left(\alpha, \frac{\sigma^0_{gr}}{\sigma^0_{veg}}, H_i\right)\right) - C_i\right]^2} \tag{10a}$$

$$\Delta\sigma\left(\alpha, \sigma^0_{gr}, \sigma^0_{veg}, \gamma_{sys}\right) = \sqrt{\frac{1}{N}\sum_{i=1}^{N}\left[\sigma_{for}\left(\alpha, \sigma^0_{gr}, \sigma^0_{veg,}, V\left(\alpha, \frac{\sigma^0_{gr}}{\sigma^0_{veg}}, H_i\right)\right) - S_i\right]^2} \tag{10b}$$

In Fig. 4 we see two backscatter values deviate from the general trend, which is the case for all of the TanDEM-X observations, and is caused by enhanced backscattering from ground sloping towards the radar. These two stands are excluded from Eq. (10b) as considered untypical for the data trend.

We want to minimize Eqs. (10a) and (10b) in such a way that the minima are obtained for the same values of the parameters, cf. Askne and Santoro (2015). In this paper this is done by means of a nonlinear minimization of $\Delta(\alpha, \sigma^0_{gr}, \sigma^0_{veg}, \gamma_{sys})$:

$$\Delta\left(\alpha, \sigma^0_{gr}, \sigma^0_{veg}, \gamma_{sys}\right) = (1-w)\Delta\gamma\left(\alpha, \sigma^0_{gr}, \sigma^0_{veg}, \gamma_{sys}\right) + w\Delta\sigma\left(\alpha, \sigma^0_{gr}, \sigma^0_{veg}, \gamma_{sys}\right) \tag{11}$$

where w is a weight factor balancing the importance of $\Delta\gamma$ versus $\Delta\sigma$. The weighting factor w is determined by requiring that the two error contributions are equal in the final solution. This imposes that:

$$(1-w)\Delta\gamma\left(\alpha, \sigma^0_{gr}, \sigma^0_{veg}, \gamma_{sys}\right) = w\Delta\sigma\left(\alpha, \sigma^0_{gr}, \sigma^0_{veg}, \gamma_{sys}\right) \tag{12}$$

We note that a minimum of $\Delta(\alpha, \sigma^0_{gr}, \sigma^0_{veg}, \gamma_{sys})$ for e.g. α is obtained simultaneously with minima for $\Delta\gamma(\alpha, \sigma^0_{gr}, \sigma^0_{veg}, \gamma_{sys})$ and $\Delta\sigma(\alpha, \sigma^0_{gr}, \sigma^0_{veg}, \gamma_{sys})$, which is a physical demand. We also note that $2/\Delta = 1/\Delta\gamma + 1/\Delta\sigma$. This means that the individual contributions of the coherence and backscatter errors will be weighted depending on their relative values. Typically $1 \le \Delta\gamma(\alpha, \sigma^0_{gr}, \sigma^0_{veg}, \gamma_{sys})/\Delta\sigma(\alpha, \sigma^0_{gr}, \sigma^0_{veg}, \gamma_{sys}) < 2.2$ except for two winter cases for which the ratio is <1. The minimization is illustrated in the complex plane in Fig. 5 for data from 2011-06-17.

The various steps are summarized as follows: h is introduced as the height of the layer with random scatterers which is assumed to be equal to the basal area weighted mean forest height. The modeled phase height z_{est} is set equal to the observed phase height and the IWCM

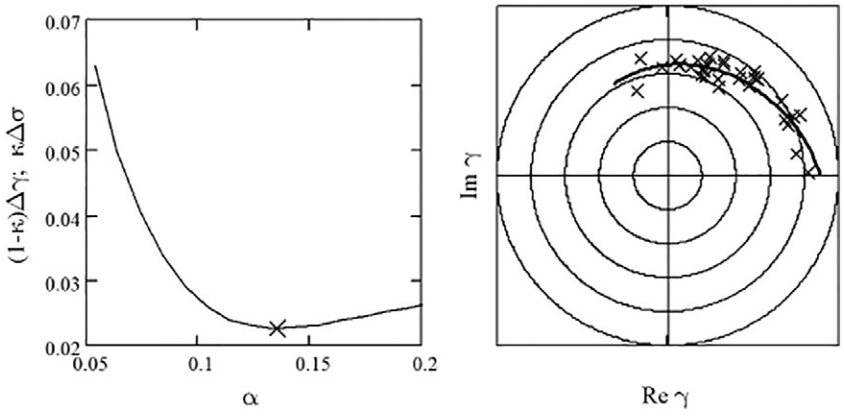

Fig. 5. Illustrating the variation of the two error functions $(1 - w)\Delta\gamma$ and $w\Delta\sigma$ (both of them equal) as function of α, and the model and observations in the complex coherence plane.

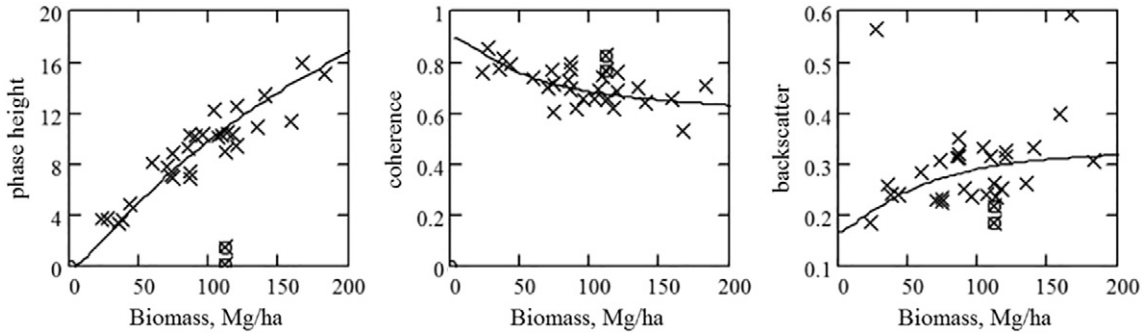

Fig. 6. The observed phase height, coherence and backscatter for 31 stands with TanDEM-X acquisition from 2011-06-17 versus the in situ biomass (x) and the derived model result. Two stands have been clear cut since the in situ observations in 2008, and are marked by encircled x; two stands have anomalous σ-values ≈ 0.6, related to slope effects. Model illustrated for $\alpha = 0.136$, $\gamma_{sys} = 0.889$, $\sigma^0_{gr} = 0.165$, and $\sigma^0_{veg} = 0.344$.

parameters are determined by fitting the model to the observations, H_i, C_i, and S_i. When the IWCM parameters are determined the stem volume, V_i, biomass, $BF \cdot V_i$, and height, $h(V_i)$ for each stand can be determined from the observed phase height of the stand.

As an example, the results for the acquisition 2011-06-17 are illustrated in Fig. 6 as function of AGB estimated from in situ measurements in 2008. The minimization method used is the nonlinear conjugate gradient method. The estimated w-values are in the range 0.45–0.70, but in two cases values in the range 0.20 and 0.25 related to high values of $\sigma^0_{gr}/\sigma^0_{veg}$ or HoA.

4.3. Winter case anomaly

For one of the investigated cases, the winter case 2012-02-25, which has a 1 m snow layer and −9 °C, the phase height/coherence and backscatter/phase height diagrams changed considerably, cf. Fig. 7. (For comparison to a typical summer cases, see Fig. 4.) After minimization the model results should be checked versus the observations. Since we are looking for systematic trends in the observations we note that we have four outliers in the backscatter/phase height diagram (two clear cuts and two influenced by topography), which affects the minimization described above. These four stands are therefore excluded from the minimization in Eqs. (10a) and (10b) as influenced by the snow layer and considered atypical. This results in a solution with $\sigma^0_{gr}/\sigma^0_{veg} = 2.7$ and $\alpha = 0.11$, see Fig. 7. The IWCM phase height, modeled for 0–200 Mg/ha, reaches 8.3 m in the original solution and 10.2 m in the second case, while the measured phase heights reach up to 10.5 m, also indicating that the second solution with $\sigma^0_{gr}/\sigma^0_{veg} = 2.7$ and $\alpha = 0.11$ is the better solution. The RMSE (29 stands) for biomass is obtained as 19.1% (28.1% for the rejected solution).

During the period 2012-02-20–2012-02-25 the temperature varies between −12 °C and +1 °C during the days and the snow layer at 6 am between 0.96 and 1.02 m. We don't know anything about possible snow in the canopy and the model, Eqs. (1)–(5b) is not adapted for snow. If the four stands are not excluded, the minimization is driven by the large spread of the backscatter values for this winter case, and with the consequence that the parameter values may lose their physical meaning. One noteworthy property in the winter case, however, is the small spread of coherence values.

There is one more acquisition from the winter season, 2013-12-27, with temperatures varying during the day between −1.3° (6 am) and −0.1 (6 pm). In this case the solution is characterized by $\sigma^0_{gr}/\sigma^0_{veg} = 0.74$ and $\alpha = 0.14$, values somewhat enhanced relative summer acquisitions.

The acquisitions studied in this paper cover mainly summer conditions and the winter cases have shown effects indicating possible complications probably depending on snow influence. Summer acquisitions are therefore preferred for biomass estimation.

5. Results

5.1. IWCM parameters

In Fig. 8 the IWCM parameters, $\sigma^o_{gr}, \sigma^o_{veg}, \alpha$, and γ_{sys} as obtained in the minimization process, are plotted against air temperature on the day of acquisition and total precipitation during the day of the acquisition and the two preceding days. The dependence of γ_{sys} on HoA is also illustrated. The winter case 2012-02-25 is uncertain due to a 1 m snow layer. We primarily observe an increase of σ^o_{veg} with temperature, which most likely is related to the water content within the vegetation. The

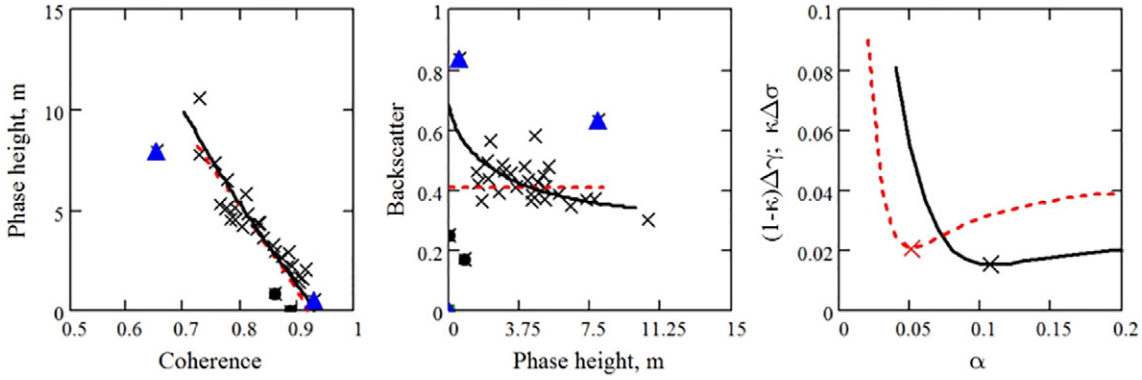

Fig. 7. Observations of the winter case 2012-02-25 with two alternative model results, summer case solution, red dotted lines with $\sigma^0_{gr}/\sigma^0_{veg} = 1.0$ and $\alpha = 0.05$, and solution with four stands believed to be affected by snow layer excluded from minimization, black solid line with $\sigma^0_{gr}/\sigma^0_{veg} = 2.7$ and $\alpha = 0.11$ (two stands affected by topography, marked by blue triangles, and two clear cut stands, marked by black boxes). Minima as function of α also illustrated.

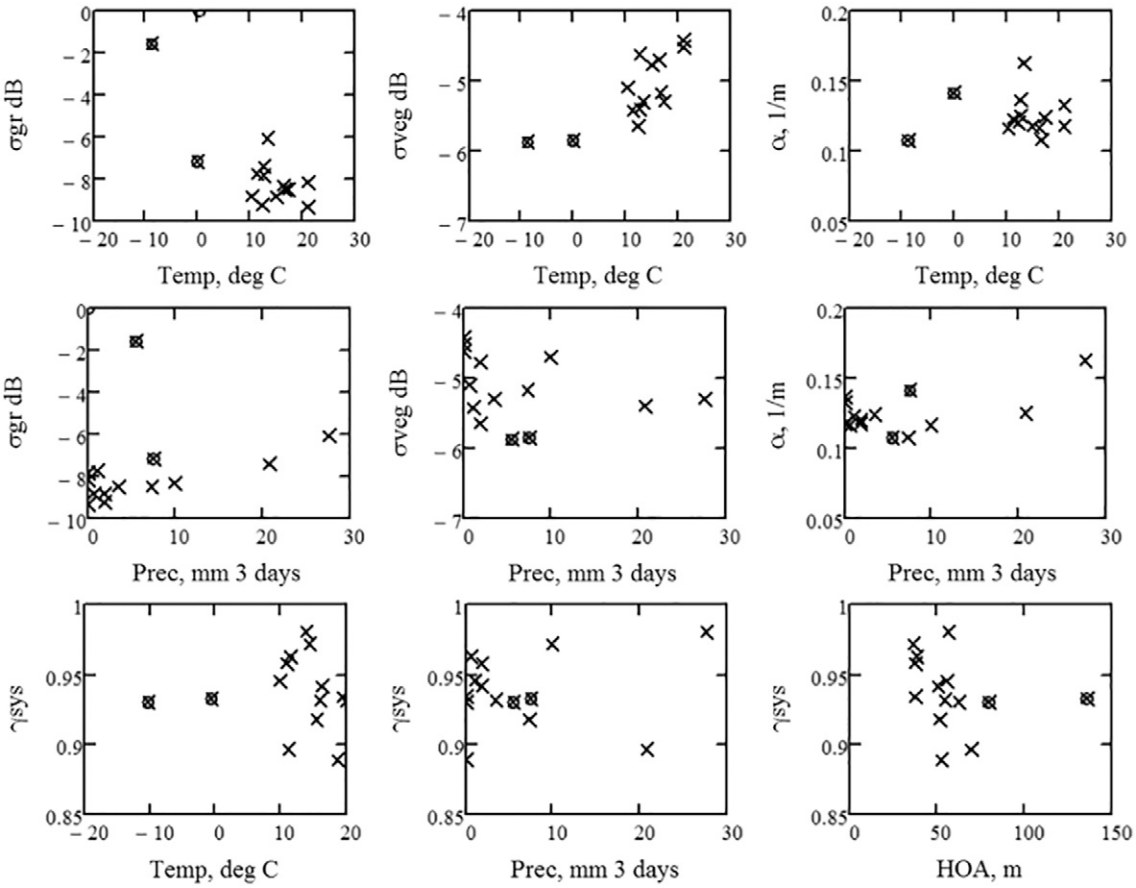

Fig. 8. Weather and HoA dependence of IWCM parameters for different TanDEM-X acquisitions. Summer times marked by x and winter time marked by encircled x, temperatures from 18 UTC.

variation of the other parameters is too uncertain for general conclusions. α, however, does not seem to be clearly related to temperature and precipitation, which may indicate that dielectric effects play less role compared to penetration through gaps to lower levels of the vegetation.

5.2. Accuracy of estimated biomass and height

The RMSE (in the paper, RMSE is defined as a percentage of the mean value), and the Pearson coefficient squared, r^2, together with bias for biomass estimated from TanDEM-X data relative biomass estimated from in situ measurements in 2008 are illustrated in Fig. 9. We note that due to the estimation process, the estimated biomass is influenced by the values of α and $\sigma^o_{gr}/\sigma^o_{veg}$, but not by γ_{sys}.

The TanDEM-X measurement closest in time to the field and ALS observations, 2011-06-17, is characterized by RMSE for biomass equal to 16.6% and for forest height equal to 11.5%, normalized by a mean biomass of 93.9 Mg/ha and a mean height of 15.1 m. The RMSE for the other observations range between 15.8 and 21.2% for biomass, as illustrated in Fig. 9, and 9.9–16.0% for height. Three measurements are characterized by no precipitation on the day of acquisition nor the two preceding days and three additional measurements characterized by

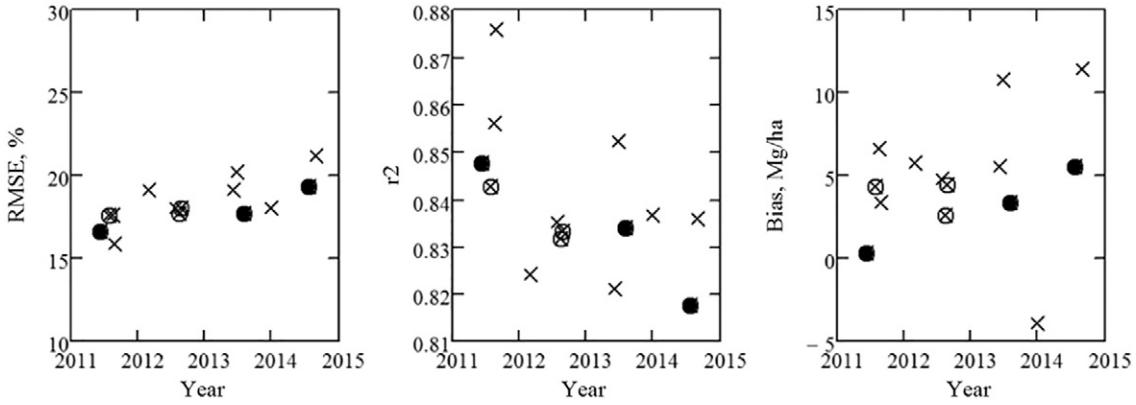

Fig. 9. RMSE, r^2, and bias for estimated biomass vs. 2008 in situ measurements. Three measurements not affected by precipitation are marked by •, while additionally three measurements are affected by limited precipitation and marked by o.

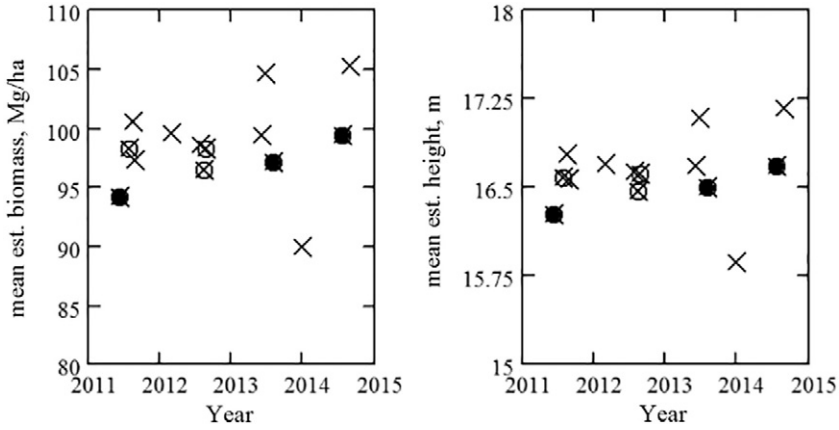

Fig. 10. Illustrating mean estimated biomass and forest height. Measurements little affected by precipitation marked as in Fig. 9.

no precipitation on the day of acquisition and <3.5 mm on the two preceding days, cf. Fig. 9. We conclude that the results are sensitive to precipitation. The increase of RMSE and bias, and the decrease of r^2 with time for the acquisition without precipitation are in line with what can be expected due to forest growth with time.

The mean biomass and forest height are illustrated in Fig. 10 and acquisitions little affected by precipitation in 72 h are marked as earlier. The scatter of the points demonstrates the stability of the estimation process. The low value for 2013-12-27 is associated with a temperature of −0.7 °C and a 6 cm snow layer. The second winter case, 2012-02-25, does not stand out after the removal of the four outliers in the minimization process. The observations from 2013-12-27 seem to be affected by the snow layer close to melting, and we conclude that winter cases with a snow layer seem less suitable for estimating biomass with the present model.

5.3. Using ALS as reference

Next, we will study the large area with ALS data as reference and for that reason we will first compare field and ALS inventory. For the investigated 29 stands we find RMSE = 18.6, r^2 = 0.87, and a bias between in situ and ALS of 9.4 Mg/ha. If the ALS observations are used as reference for the estimated biomass by means of TanDEM-X we obtain the results in Fig. 11.

From Fig. 11 we note higher level and scattering of the RMSE values, and higher bias, but less scattered and higher values for r^2 (0.91–0.94 with the exception of a winter case). The results indicate that TanDEM-X and ALS have similar measurements properties (high r^2), but the TanDEM-X measurements are better calibrated (less bias) in spite of no local training data in IWCM (but optimized for the relevant stands) while for the interpretation of the ALS measurements local training data have been used (but for a larger area).

5.4. Large area with ALS as reference

The interferometric water cloud model has been applied to 29 stands for which in situ data are available and therefore suitable for testing the accuracy of the model and its solution. However, the ALS measurements cover a large area, and the TanDEM-X investigation will now be extended to the same area. We will concentrate on the acquisition from 2011-06-17, closest in time to the ALS observations in August 2008. Within the covered area consisting of 1071 stands, we analyze the 646 forest stands with an area larger than 1 ha in order to stabilize forest properties. In order to compare with the ALS measurements we exclude 27 stands with large changes detected using a simple comparison between the measured phase height and ALS biomass (phase height in m < 0.03 of the ALS biomass in Mg/ha). Using aerial photography, these changes can be verified to be man-made and caused by harvesting. The remaining 619 stands cover an area of 3166 ha out of the total area of 3535 ha for 646 stands. Over this large area, forest properties vary somewhat more than in the case of the 29 reference stands, as illustrated in Fig. 12. In particular, we see a larger variability in backscatter. The minimization procedure took place over the 619 stands and w was found to be small due to the large spread in the backscatter. We obtain w = 0.127 and RMSE = 18.4% and bias = 1.1 Mg/ha using ALS as reference (mean biomass 76.9 Mg/ha). The model solution is shown in Fig. 12.

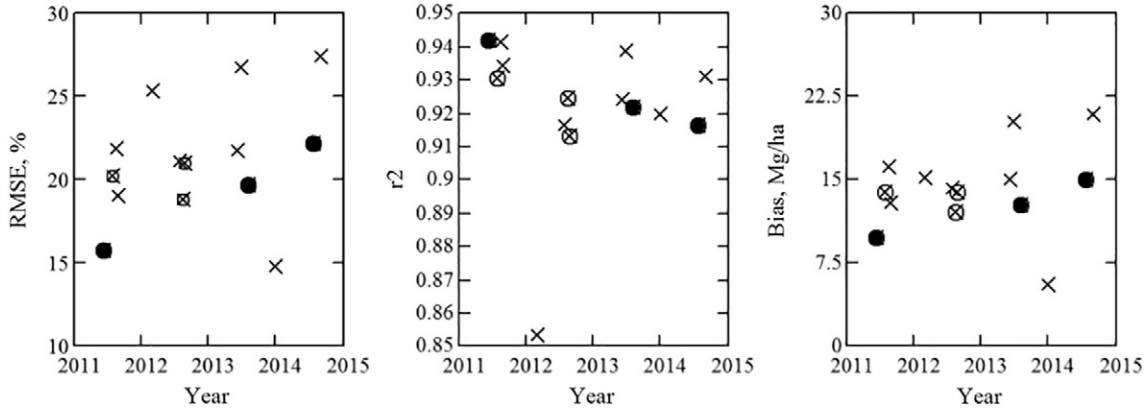

Fig. 11. RMSE, r^2, and bias for estimated biomass vs. 2008 ALS measurements. Measurements little affected by precipitation marked as in Fig. 9.

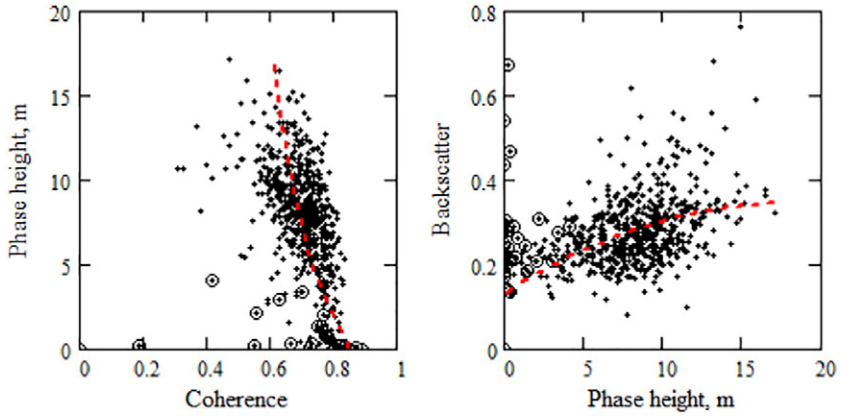

Fig. 12. TanDEM-X data (2011-06-17) from 646 stands >1 ha. Those 27 stands assumed to have changed since ALS measurements in August 2008 are marked by o. The model solution is shown as a red dashed line.

Diagrams with the estimated biomass versus the ALS biomass are shown in Fig. 13. In the biomass comparison diagram, the 27 stands assumed to have changed are marked. The histogram of all 1071 stands illustrates the change of biomass.

The two-level model (TLM) introduced in Soja et al. (2015b) models forest as two scattering levels, ground and vegetation, the latter with gaps. By fitting this two-parameter model to measured coherence and phase height, metrics related to forest height and vegetation density are obtained simultaneously, for each pixel, and without model training. The derived vegetation density is illustrated in Fig. 14 for the forest stands together with the above derived biomass. The vegetation density like measure is also compared with the vegetation ratio for the stands. We conclude that the allometric relation for the area-fill is in good agreement with the vegetation density measure expecting area-fill to be higher than vegetation ratio, cf. Section 4.1.

5.5. Using phase height as reference for biomass

The model solution for biomass was determined from the phase height while the model parameters, which determine the modeled

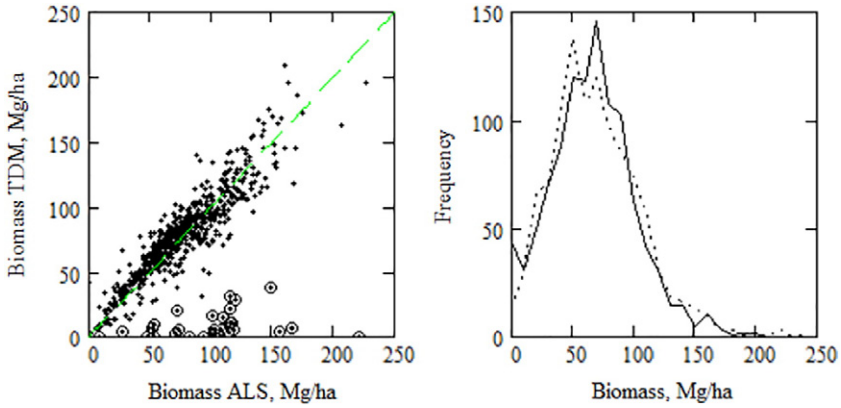

Fig. 13. Estimated biomass (2011-06-17) vs. ALS biomass (August 2008), 646 stands >1 ha with those assumed to be changed in the time period between ALS and TanDEM-X marked with o. The histogram shows the estimated biomass (solid line) compared to the ALS biomass (dashed line) for all 1071 stands.

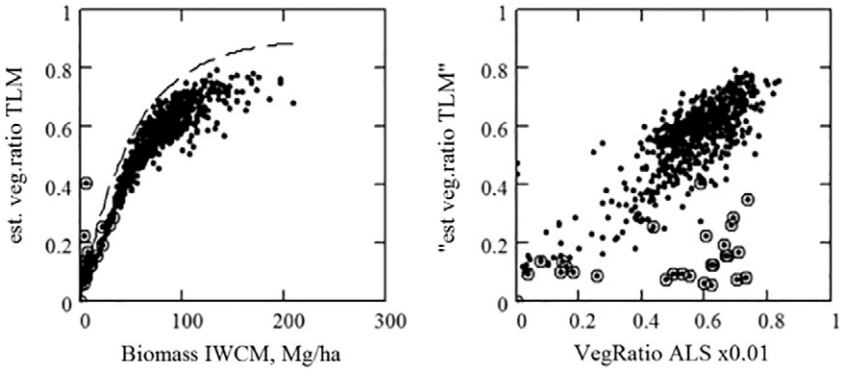

Fig. 14. Results for 2011-06-17, 646 stands >1 ha of the vegetation density measure derived by TLM, compared with the allometric relations (6), (8) and with the ALS vegetation density. 27 stands classified as changed relative 2008 marked by o.

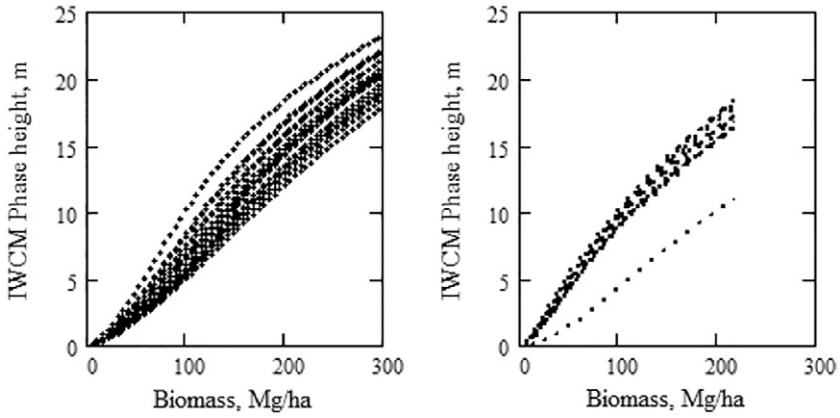

Fig. 15. Left). Modeled phase height in Remningstorp (Askne et al., 2013), and right) in Krycklan illustrating the trends in the relation between phase height and biomass. (The rather low phase height curve for Krycklan is the winter case 2012-02-25.)

phase height, were determined from the properties of coherence and backscatter. In the end we find a functional relation between phase height and biomass, see Fig. 15, where also the results from Remningstorp (Askne et al., 2013) have been included.

The main difference between Remningstorp and Krycklan is the value of $\sigma^0_{gr}/\sigma^0_{veg}$, which in the case of Remningstorp is >1 (probably due to high soil moisture) and for Krycklan is <1 except for the winter case with 1 m snow layer. When $\sigma^0_{gr}/\sigma^0_{veg} > 1$ the phase height will decrease for low biomass values due to the influence of ground scattering. (In the winter case 2012-02-25 from Krycklan with $\sigma^0_{gr}/\sigma^0_{veg} = 2.7$ this influence is so strong that the entire biomass range is affected.)

5.6. Large area coverage, AGB(PH)

The obtained solution for the phase height, z_{est}, versus AGB can be inverted to a relation for AGB as function of phase height e.g. by means of a lookup table or a polynomial expression. The ALS-covered area in Krycklan is illustrated in Fig. 16, where biomass over the investigated area is increasing from white (zero biomass) to deep green (300 Mg/ha). The pixel size is 12 m (the scene center resolutions of TanDEM-X 2011-06-17 is 1.8 m in ground range and 6.6 m in azimuth).

Fig. 17 shows the three-year change between the TanDEM-X and ALS estimates of biomass. Areas with decreased biomass are

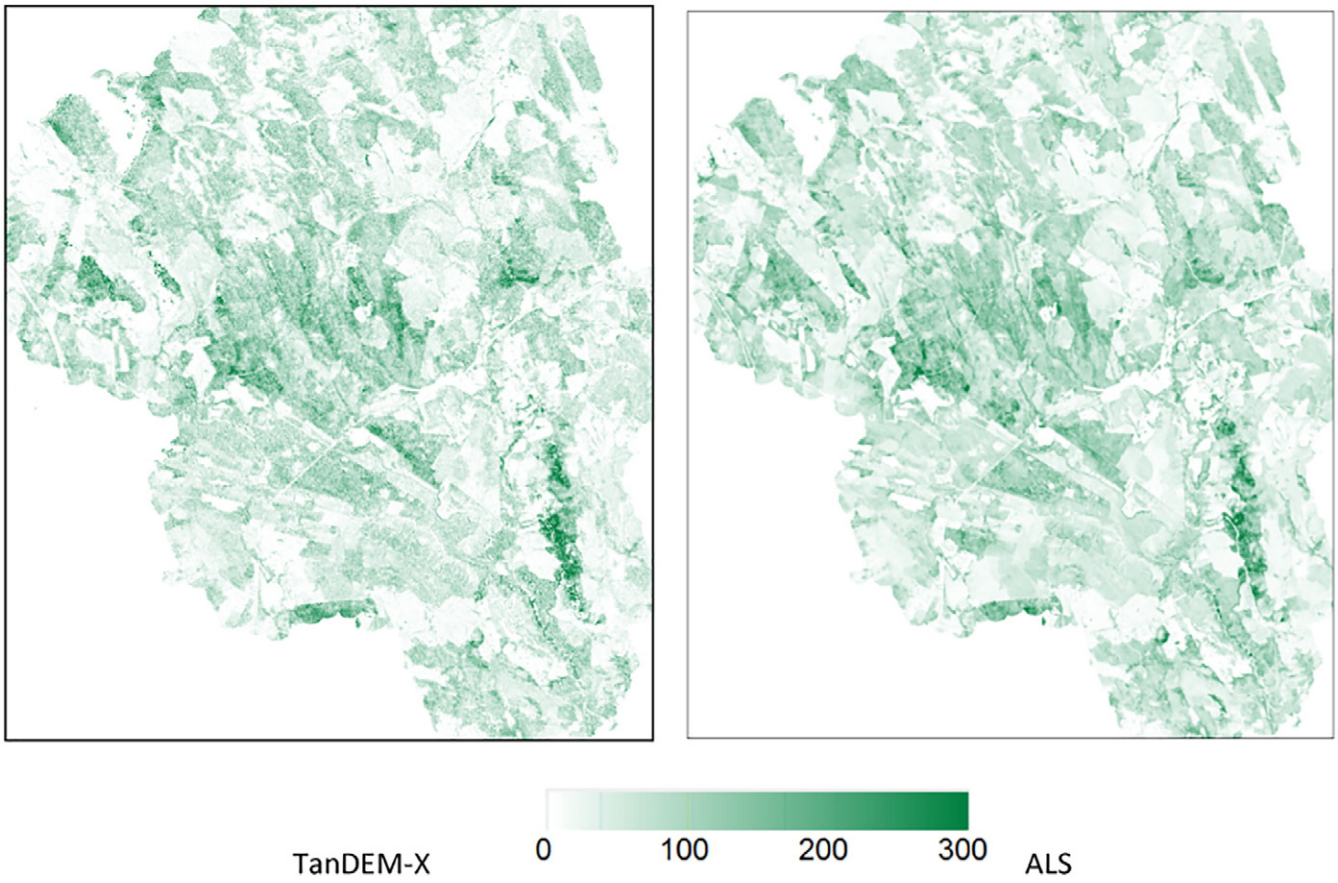

Fig. 16. Biomass maps of the Krycklan test area. Zero biomass is represented by white, while 300 Mg/ha is represented by deep green. Area: ≈10.1 × 11.5 km^2. TanDEM-X acquisition from 2011-06-17, ALS from August 2008.

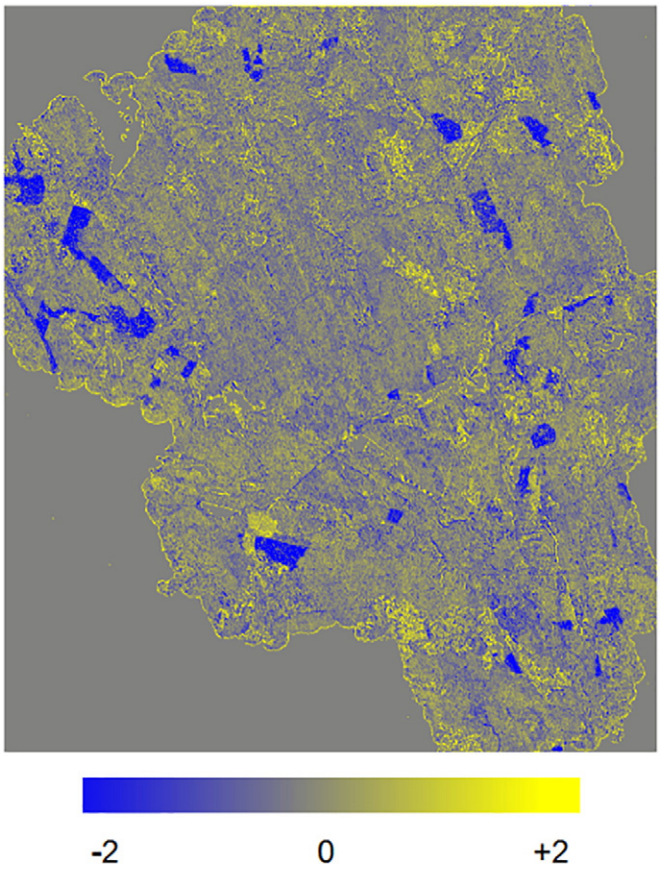

Fig. 17. Biomass change map between ALS from August 2008 and TanDEM-X from June 2011. The map shows the (natural) logarithmic ratio between biomass from TanDEM-X and ALS, i.e. $-2 \le \ln(\text{ratio}) \le 2$ with a decrease of biomass in blue, and increase in yellow.

represented by blue tones (clear cut or thinned stands) while areas with large growth represented by yellow tones (young stands). Normal growth is represented by grey tones. Due to the different geometries of ALS (nadir looking) and TanDEM-X (42° incidence angle) roads surrounded by forest will often be enhanced. Similar effects will appear at boundaries between forest and open fields. Effects related to topography and the difference in incidence angle between ALS and TanDEM-X can also be seen.

6. Discussion and conclusion

Forest height is a quantity directly measureable by remote sensing, but stem volume is more complex to determine since sensitivity for the stem diameter is needed. VHF-band radar has such sensitivity (Smith-Jonforsen et al., 2005; Smith and Ulander, 2000). To determine AGB is still more complex since it is related to wood density and the non-woody fraction of the biomass. No remote sensing technique is available for direct measurements of AGB.

High microwave frequencies, such as X- and C-band, are mainly sensitive to the upper layer in a dense forest and only affected by the ground conditions for less dense areas. Phase height from bistatic interferometric measurements, after removal a DTM, is closely related to forest height and density, and therefore also to AGB. The differences in measurements relative low frequencies, such as VHF- and P-band, make X- and C-band suitable for complementary use.

To interpret remote sensing observations a model has to be used and parameters determined, and it is important for the model to include effects of height and density. Different approaches are used; e.g. IWCM, TLM (Soja et al., 2015a), PolInSAR, often combined with RVoG (Cloude and Papathanassiou, 1998; Cloude and Papathanassiou, 2003; Papathanassiou and Cloude, 2001; Treuhaft et al., 1996), multi-baseline, tomographic PolInSAR (Toraño Caicoya et al., 2015), statistical approaches like Random-Forest (Karila et al., 2015), relating observations to known conditions, etc. Most approaches are based on the knowledge of local training data; others are related to complex sensor technique demanding polarimetry or tomography.

In this paper we investigated properties of bistatic TanDEM-X measurements for a boreal test site. IWCM has been applied to single-polarized (VV), single-baseline TanDEM-X data using an available DTM as ground reference for phase height estimation. No corrections of the observations for topography except in normalizing the backscattering coefficients have been done. Further research should analyze errors in the biomass estimation with topography and incidence angle in particular with snow layers.

The model has been fitted to three TanDEM-X observables: phase height, coherence, and backscatter. Allometric functions are used to assure the proper inter-dependence between forest parameters such as forest height, canopy cover, AGB, and stem volume. Allometric functions describe the mean properties rather than properties of individual forest stands, and are therefore most suitable for inclusion in a model like IWCM, describing the mean properties of the observed quantities (phase height, coherence and backscatter).

The phase height, coherence, and backscatter for the 31 stands with in situ data are shown to be stable over the three-year-period, in particular the phase height, which is the TanDEM-X measurement most correlated with AGB. For AGB, the RMSE 2011–2014 varies between 15.8 and 21.2%, increasing with time from the in situ reference in 2008. The RMSE for height relative to the basal area weighted mean height similarly varies between 9.9 and 16.0%.

In situ data have been used as reference data in this paper, but ALS data are also available for the entire test site. The ALS estimated biomass of the 29 stands have an accuracy of 18.6% and a height accuracy of 9% relative in situ estimates, and we conclude that ALS (using local training data) and TanDEM-X (not using local training data) have similar uncertainties. The AGB for 619 stands >1 ha with biomass up to 291 Mg/ha and covering 3166 ha was also estimated for one TanDEM-X acquisition with RMSE = 18.3% ($r^2 = 0.83$) compared to ALS. The AGB change for the entire area ($\approx$68 km^2) clearly delineates changes corresponding to clear cuts and high growth in low biomass areas.

The Interferometric Water Cloud Model, sensitive to forest height as well as vegetation density, can be used for single polarization TanDEM-X observations for accurate estimation of AGB and forest height in Swedish boreal forests without the use of local training data but using allometry (6)–(8). A DTM is assumed to be known, which is also the case for Sweden, along with a number of other countries. Without the DTM, only coherence and backscatter are available (Olesk et al., 2016; Olesk et al., 2015; Toraño Caicoya et al., 2016). IWCM has also been applied to the hemi-boreal test site Remningstorp, 720 km south Krycklan (Askne et al., 2013; Askne and Santoro, 2015), and in order to apply IWCM to areas with different forest characteristics the model Eqs. (1)–(5b) must be considered applicable. In this paper $h(V)$ was given based on investigation of 3046 NFI-plots for Sweden and expressions can be found in the literature for various other areas, for $h(V)$ or $h(B)$, see e.g. Cartus et al. (2012), Mette et al. (2004), Saatchi et al. (2011), and Santoro et al. (2007), for $\eta(V)$, see e.g. Cartus and Santoro (2016), Cartus et al. (2012), and Cartus et al. (2011), and for BF, see e.g. Thurner et al. (2013). The area-fill expression can be checked by a combination the vegetation density like quantity derived by a TLM-analysis of the TanDEM-X data and the biomass derived with the presented method.

The high accuracy is mainly due to the relatively simple relation between phase height and biomass, although this relation varies with environmental conditions and HoA. The good results derived from bistatic TanDEM-X observations motivates continued use of a bistatic high frequency InSAR mission, complementing the BIOMASS P-band mission,

which may provide a DTM to be used in estimating the X-band phase height.

Acknowledgement

ESA and the BioSAR 2008 team are gratefully acknowledged for funding and collecting the forest ground data. DLR is acknowledged for TanDEM-X data distributed through proposal XTI_VEG0376 3D Forest Parameter Retrieval from TanDEM-X Interferometry (L.M.H. Ulander PI). This work was partly funded by the Swedish National Space Board Grant 269/14.

References

Askne, J., Santoro, M., 2012. Experiences in boreal forest stem volume estimation from multitemporal C-band InSAR. In: Padron, I. (Ed.), Recent Interferometry Applications in Topography and Astronomy. InTech Open Access Publisher, pp. 169–194.
Askne, J.I.H., Santoro, M., 2015. On the estimation of boreal forest biomass from TanDEM-X data without training samples. IEEE Geosci. Remote Sens. Lett. 12, 771–775.
Askne, J., Dammert, P., Ulander, L.M.H., Smith, G., 1997. C-band repeat-pass interferometric SAR observations of the forest. IEEE Trans. Geosci. Remote Sens. 35, 25–35.
Askne, J., Santoro, M., Smith, G., Fransson, J.E.S., 2003. Multitemporal repeat-pass SAR interferometry of boreal forests. IEEE Trans. Geosci. Remote Sens. 41, 1540–1550.
Askne, J.I.H., Fransson, J.E.S., Santoro, M., Soja, M.J., Ulander, L.M.H., 2013. Model-based biomass estimation of a hemi-boreal forest from multitemporal TanDEM-X acquisitions. Remote Sens. 5, 5574–5597.
Attema, E.P.W., Ulaby, F.T., 1978. Vegetation modelled as a water cloud. Radio Sci. 13, 357–364.
Cartus, O., Santoro, M., 2016. Multi-scale mapping of forest growing stock volume using ENVISAT ASAR, ALOS PALSAR, Landsat, and ICESAT GLAS. ESA Living Planet Symposium. ESA, Prague.
Cartus, O., Santoro, M., Schmullius, C., Li, Z., 2011. Large area forest stem volume mapping in the boreal zone using synergy of ERS-1/2 tandem coherence and MODIS vegetation continuous fields. Remote Sens. Environ. 115, 931–943.
Cartus, O., Santoro, M., Kellndorfer, J., 2012. Mapping forest aboveground biomass in the Northeastern United States with ALOS PALSAR dual-polarization L-band. Remote Sens. Environ. 124, 466–478.
Cloude, S.R., Papathanassiou, K.P., 1998. Polarimetric SAR interferometry. IEEE Trans. Geosci. Remote Sens. 36, 1151–1165.
Cloude, S.R., Papathanassiou, K.P., 2003. A 3-stage inversion process for polarimetric SAR interferometry. IEE Proc. Radar Sonar. Navig. 150, 125–134.
ESA, 2012. BIOMASS - Report for Mission Selection - An Earth Explorer to Observe Forest Biomass. European Space Agency, Noordwijk, The Netherlands, p. 193.
Hagberg, J.O., Ulander, L.M.H., Askne, J., 1995. Repeat-pass SAR interferometry over forested terrain. IEEE Trans. Geosci. Remote Sens. 33, 331–340.
Hajnsek, I., Scheiber, R., Keller, M., Horn, R., Lee, S., Ulander, L., Gustavsson, A., Sandberg, G., Toan, T.L., Tebaldini, S., Guarnier, A.M., Rocca, F., 2009. BIOSAR 2008 Technical Assistance for the Development of Airborne SAR and Geophysical Measurements during the BioSAR 2008 Experiment, Final Report. ESA contract No. 22052/08/NL/CT. Available:. https://earth.esa.int/c/document_library/get_file?folderId=21020&name=DLFE-21903.pdf.
Holmgren, J., 2004. Prediction of tree height, basal area and stem volume in forest stands using airborne laser scanning. Scand. J. For. Res. 19, 543–553.
Holmgren, J., Nilsson, M., Olsson, H., 2003. Estimation of tree height and stem volume on plots using airborne laser scanning. For. Sci. 49, 419–428.
Houghton, R.A., Hall, F., Goetz, S.J., 2009. Importance of biomass in the global carbon cycle. J. Geophys. Res. Biogeosci. 2005–2012, 114.
Kaasalainen, S., Holopainen, M., Karjalainen, M., Vastaranta, M., Kankare, V., Karila, K., Osmanoglu, B., 2015. Combining lidar and synthetic aperture radar data to estimate forest biomass: status and prospects. Forests 6, 252–270.
Karila, K., Vastaranta, M., Karjalainen, M., Kaasalainen, S., 2015. Tandem-X interferometry in the prediction of forest inventory attributes in managed boreal forests. Remote Sens. Environ. 159, 259–268.
Korhonen, L., Korpela, I., Heiskanen, J., Maltamo, M., 2011. Airborne discrete-return LIDAR data in the estimation of vertical canopy cover, angular canopy closure and leaf area index. Remote Sens. Environ. 115, 1065–1080.
Krieger, G., Moreira, A., Fiedler, H., Hajnsek, I., Werner, M., Younis, M., Zink, M., 2007. TanDEM-X: a satellite formation for high-resolution SAR interferometry. IEEE Trans. Geosci. Remote Sens. 45, 3317–3341.
Kugler, F., Schulze, D., Hajnsek, I., Pretzsch, H., Papathanassiou, K.P., 2014. TanDEM-X Pol-InSAR performance for forest height estimation. IEEE Trans. Geosci. Remote Sens. 52, 6404–6422.
Le Toan, T., Quegan, S., Davidson, M.W.J., Balzter, H., Paillou, P., Plummer, S., Papathanassiou, K., Rocca, F., Saatchi, S., Shugart, H., Ulander, L.M.H., 2011. The BIOMASS mission: mapping global forest biomass to better understand the terrestrial carbon cycle. Remote Sens. Environ. 115, 2850–2860.
Lefsky, M.A., Cohen, W.B., Harding, D.J., Parker, G.G., Acker, S.A., Gower, S.T., 2002. Lidar remote sensing of above-ground biomass in three biomes. Glob. Ecol. Biogeogr. 11, 393–399.
Li, X., Strahler, A.H., 1985. Geometric-optical modeling of a conifer forest canopy. IEEE Trans. Geosci. Remote Sens. 705–721.
Liu, J., Woodcock, C.E., Melloh, R.A., Davis, R.E., McKenzie, C., Painter, T.H., 2008. Modeling the view angle dependence of gap fractions in forest canopies: implications for mapping fractional snow cover using optical remote sensing. J. Hydrometeorol. 9, 1005–1019.
Mette, T., Papathanassiou, K., Hajnsek, I., 2004. Biomass estimation from polarimetric SAR interferometry over heterogeneous forest terrain. IGARSS 2004. IEEE, pp. 511–514.
Næsset, E., 2002. Predicting forest stand characteristics with airborne scanning laser using a practical two-stage procedure and field data. Remote Sens. Environ. 80, 88–99.
Neumann, M., Saatchi, S.S., Ulander, L.M.H., Fransson, J.E.S., 2012. Assessing performance of L-and P-band polarimetric interferometric SAR data in estimating boreal forest above-ground biomass. IEEE Trans. Geosci. Remote Sens. 50, 714–726.
Olesk, A., Voormansik, K., Vain, A., Noorma, M., Praks, J., 2015. Seasonal differences in forest height estimation from interferometric TanDEM-X coherence data. IEEE JSTARS 8, 5565–5572.
Olesk, A., Praks, J., Antropov, O., Zalite, K., Arumäe, T., Voormansik, K., 2016. Interferometric SAR coherence models for characterization of hemiboreal forests using TanDEM-X data. Remote Sens. 8, 700.
Papathanassiou, K.P., Cloude, S.R., 2001. Single-baseline polarimetric SAR interferometry. IEEE Trans. Geosci. Remote Sens. 39, 2352–2363.
Persson, H., Fransson, J.E.S., 2014. Forest variable estimation using radargrammetric processing of TerraSAR-X images in boreal forests. Remote Sens. 6, 2084–2107.
Persson, H.J., Fransson, J.E.S., 2016. Comparison between TanDEM-X-and ALS-based estimation of aboveground biomass and tree height in boreal forests. Scand. J. For. Res. 1–14.
Persson, H., Wallerman, J., Olsson, H., Fransson, J.E., 2013. Estimating forest biomass and height using optical stereo satellite data and a DTM from laser scanning data. Can. J. Remote. Sens. 39, 251–262.
Petersson, H., 1999. Biomassafunktioner för trädfraktioner av tall, gran och björk i Sverige (in Swedish with English summary). Department of Forest Resource Management, Swedish University of Agricultural Sciences, Umeå, Sweden.
Rodriguez, E., Martin, J.M., 1992. Theory and design of interferometric synthetic aperture radars. IEE Proc. F 139, 147–159.
Saatchi, S.S., Harris, N.L., Brown, S., Lefsky, M., Mitchard, E.T.A., Salas, W., Zutta, B.R., Buermann, W., Lewis, S.L., Hagen, S., 2011. Benchmark map of forest carbon stocks in tropical regions across three continents. Proc. Natl. Acad. Sci. 108, 9899–9904.
Santoro, M., Askne, J., Smith, G., Fransson, J.E.S., 2002. Stem volume retrieval in boreal forests from ERS-1/2 interferometry. Remote Sens. Environ. 81, 19–35.
Santoro, M., Askne, J., Dammert, P., 2005. Tree height influence on ERS interferometric phase in boreal forest. IEEE Trans. Geosci. Remote Sens. 43, 207–217.
Santoro, M., Shvidenko, A., McCallum, I., Askne, J., Schmullius, C., 2007. Properties of ERS-1/2 coherence in the Siberian boreal forest and implications for stem volume retrieval. Remote Sens. Environ. 106, 154–172.
Santoro, M., Beer, C., Cartus, O., Schmullius, C., Shvidenko, A., McCallum, I., Wegmüller, U., Wiesmann, A., 2011. Retrieval of growing stock volume in boreal forest using hyper-temporal series of Envisat ASAR ScanSAR backscatter measurements. Remote Sens. Environ. 115, 490–507.
Santoro, M., Beaudoin, A., Beer, C., Cartus, O., Fransson, J.E.S., Hall, R.J., Pathe, C., Schmullius, C., Schepaschenko, D., Shvidenko, A., 2015. Forest growing stock volume of the northern hemisphere: spatially explicit estimates for 2010 derived from Envisat ASAR. Remote Sens. Environ. 168, 316–334.
Smith, G., Ulander, L.M.H., 2000. A model relating VHF-band backscatter to stem volume of coniferous boreal forest. IEEE Trans. Geosci. Remote Sens. 38, 728–740.
Smith-Jonforsen, G., Ulander, L.M.H., Luo, X., 2005. Low VHF-band backscatter from coniferous forests on sloping terrain. IEEE Trans. Geosci. Remote Sens. 43, 2246–2260.
Soja, M.J., Sandberg, G., Ulander, L.M.H., 2013. Regression-based retrieval of boreal forest biomass in sloping terrain using P-band SAR backscatter intensity data. IEEE Trans. Geosci. Remote Sens. 51, 2646–2665.
Soja, M.J., Persson, H., Ulander, L.M.H., 2015a. Estimation of forest biomass from two-level model inversion of single-pass InSAR data. IEEE Geosci. Remote Sens. Trans. 53, 5083–5099.
Soja, M.J., Persson, H., Ulander, L.M.H., 2015b. Estimation of forest height and canopy density from a single InSAR correlation coefficient. Geosci. Remote Sens. Lett. 12, 646–650.
Solberg, S., Astrup, R., Bollandsås, O.M., Næsset, E., Weydahl, D.J., 2010a. Deriving forest monitoring variables from X-band InSAR SRTM height. Can. J. Remote. Sens. 36, 68–79.
Solberg, S., Astrup, R., Gobakken, T., Næsset, E., Weydahl, D.J., 2010b. Estimating spruce and pine biomass with interferometric X-band SAR. Remote Sens. Environ. 114, 2353–2360.
Solberg, S., Astrup, R., Breidenbach, J., Nilsen, B., Weydahl, D., 2013. Monitoring spruce volume and biomass with InSAR data from TanDEM-X. Remote Sens. Environ. 139, 60–67.
Sun, G., Ranson, K.J., 2009. Forest biomass retrieval from lidar and radar. 2009 IEEE International Geoscience and Remote Sensing Symposium. IEEE, pp. V-300–V-303.
Tebaldini, S., Rocca, F., 2012. Multibaseline polarimetric SAR tomography of a boreal forest at P-and L-bands. IEEE Trans. Geosci. Remote Sens. 50, 232–246.
Thurner, M., Beer, C., Santoro, M., Carvalhais, N., Wutzler, T., Schepaschenko, D., Shvidenko, A., Kompter, E., Ahrens, B., Levick, S.R., Schmullius, C., 2013. Carbon stock and density of northern boreal and temperate forests. Glob. Ecol. Biogeogr. 23 (3), 297–310.
Toraño Caicoya, A., Pardini, M., Hajnsek, I., Papathanassiou, K., 2015. Forest above-ground biomass estimation from vertical reflectivity profiles at L-band. IEEE Geosci. Remote Sens. Lett. 12, 2379–2383.
Toraño Caicoya, A., Kugler, F., Hajnsek, I., Papathanassiou, K.P., 2016. Large-scale biomass classification in boreal forests with TanDEM-X data. IEEE Trans. Geosci. Remote Sens. 54, 5935–5951.

Treuhaft, R.N., Madsen, S.N., Moghaddam, M., vanZyl, J.J., 1996. Vegetation characteristics and underlying topography from interferometric data. Radio Sci. 31, 1449–1495.
Treuhaft, R., Goncalves, F., dos Santos, J.R., Keller, M., Palace, M., Madsen, S.N., Sullivan, F., Graça, P.M.L.A., 2015. Tropical-forest biomass estimation at X-band from the spaceborne TanDEM-X interferometer. IEEE Geosci. Remote Sens. Lett. 12, 239–243.
Ulander, L.M.H., 1996. Radiometric slope correction of synthetic-aperture radar images. IEEE Trans. Geosci. Remote Sens. 34, 1115–1122.
Ulander, L.M.H., Hagberg, J.O., Askne, J., 1994. ERS-1 SAR interferometry over forested terrain. Proceedings of the Second ERS-1 Symposium. ESA, Hamburg, pp. 475–480.